Available online at www.sciencedirect.com
SCIENCE DIRECT
Polymer 46 (2005) 10279–10289
polymer
www.elsevier.com/locate/polymer

The relation between rheological and mechanical properties of PA6 nano- and micro-composites

D.P.N. Vlasveld[a,b], M. de Jong[a], H.E.N. Bersee[c], A.D. Gotsis[a,b,1], S.J. Picken[a,b,*]

[a]*Polymer Materials and Engineering, Faculty of Applied Sciences, Delft University of Technology, Julianalaan 136, 2628 BL Delft, The Netherlands*
[b]*Dutch Polymer Institute, John F. Kennedylaan 2, P.O. Box 902, 5600 AX, Eindhoven, The Netherlands*
[c]*Design and Production of Composite Structures, Faculty of Aerospace Engineering, Delft University of Technology, Kluyverweg 3, P.O. Box 5058, 2600 GB Delft, The Netherlands*

Received 4 May 2005; received in revised form 28 July 2005; accepted 1 August 2005
Available online 22 August 2005

Abstract

A series of nanocomposites was prepared with two different methods leading to different levels of exfoliation, and the dynamic properties were measured in the solid state and the melt. The results were compared with micro-composites containing various shapes of glass filler. The higher modulus of nanocomposites at higher concentrations is accompanied by an increase in melt viscosity and the occurrence of a yield stress in the melt. The modulus at room temperature and the melt viscosity are influenced by the aspect ratio and the concentration of the filler particles. These results were used to calculate the aspect ratios of the reinforcement using the Halpin–Tsai composite model and several modified Einstein viscosity models. The experiments showed that the Simha theory for oblate and prolate spheroids predicts platelet aspect ratios from melt viscosity data that are close to the results from the Halpin–Tsai composite model and from TEM observations. The results of the analysis show the advantages and disadvantages of the various shapes and sizes of fillers and the level of exfoliation, both from a processing and a mechanical properties point of view.

Keywords: Nanocomposite; Modulus; Viscosity

1. Introduction

Particle reinforced polymer composites or compounds have been used for decades to increase the stiffness and strength of polymers and to reduce thermal expansion. Polymer nanocomposites based on exfoliated layered silicates have been developed more recently [1–3] for improved mechanical properties, barrier properties and reduced flammability. Compared to composites containing larger dispersed particles, nanocomposites have the advantage of achieving the optimal properties at relatively low filler content, resulting in a lower density and better surface smoothness and transparency. This is due to the large aspect ratio and high stiffness of the particles, resulting from the exfoliation of the layered silicate particles.

The advantages in mechanical properties of nanocomposites, such as the higher modulus and yield stress, are usually accompanied by an increase in melt viscosity and a change in rheological behaviour. The higher melt viscosity is a disadvantage for processing techniques such as extrusion and injection moulding, although it can be beneficial for film extrusion.

Both the modulus and the viscosity are influenced by the same particle related parameters, such as the particle shape and concentration; therefore, some relations between the modulus, the viscosity and the particle shape and concentration are discussed below.

1.1. Modulus of elasticity

The modulus of a layered silicate nanocomposite is dependent on the modulus and the volume fractions of the

* Corresponding author. Address: Polymer Materials and Engineering, Faculty of Applied Sciences, Delft University of Technology, Julianalaan 136, 2628 BL Delft, The Netherlands. Tel.: +31 15 2786946; fax: +31 15 2787415.
E-mail address: s.j.picken@tnw.tudelft.nl (S.J. Picken).
[1] Present address: Faculty of Sciences, Technical University of Crete, 73100 Chania, Greece.

0032-3861/$ - see front matter © 2005 Elsevier Ltd. All rights reserved.
doi:10.1016/j.polymer.2005.08.002

components and on the degree of exfoliation of the silicate particles. Improved exfoliation increases the amount of particles and their aspect ratio, the width divided by the thickness. The importance of the aspect ratio was already known for fibre composites, in which longer fibres also lead to better properties. This is even more important for nanocomposites because the volume fractions are relatively low. Many composite models take the aspect ratio into account [4–8]. Kuelpmann et al. [5] have used the Halpin–Tsai theory, Wu et al. [6] have used the Halpin–Tsai and Guth theory, and Sheng et al. [7], Fornes et al. [4] and Van Es et al. [8] have used both the Mori–Tanaka and the Halpin–Tsai theories. All these theories can be used for fibres and platelets; the Mori–Tanaka theory approximates the particles with oblate and prolate ellipsoids and the Halpin–Tsai equations uses cylinders in which the length is either larger of smaller than the diameter. Kuelpmann et al., Sheng et al. and Fornes et al. have used image analysis of SEM and TEM images to estimate the particle size distribution. Some variation between the Halpin–Tsai models used in the mentioned articles can be found in the shape-factor; some use the same factor for fibres and platelets (2* aspect ratio), while others have found that this does not give correct results for platelets [6,8]. We have chosen to use the semi-empirical Halpin–Tsai model (Eq. (1)), originally developed to describe semi-crystalline polymers [9,10], with the shape factors derived by Van Es [8]. With the appropriate shape factors for different particles shapes and orientations it can describe Young's and shear moduli. The specific shape factors can be determined by comparing the model with experimental results or with more fundamental theories i.e. the Eshelby theory, the Mori–Tanaka theory and 3D finite element modelling [7,8,11].

$$\frac{E_c}{E_m} = \frac{1 + \varsigma\eta\phi_f}{1 - \eta\phi_f} \text{ in which } \eta = \frac{(E_f/E_m) - 1}{(E_f/E_m) + \varsigma} \tag{1}$$

E_c, composite Young's modulus; E_f, Filler modulus, E_m, matrix modulus; ς, shape factor, depending on geometry, aspect ratio and orientation; ϕ_f, Filler volume fraction.

The shape factors for the tensile moduli of platelet reinforced composites are [8]:

$$\varsigma = \frac{2}{3}\left(\frac{a}{b}\right)$$

(in the radial direction of the platelets, E_{11} or E_{22})

$$\zeta = 2 \quad \text{(perpendicular to the platelets, } E_{33})$$

(a, longest dimension; b, shortest dimension).

The shape factors for fibres are [8]:

E_{11} or E_{22} $\quad \zeta = 2$ (perpendicular to the fibre direction)

E_{33} $\quad \zeta = 2\left(\frac{a}{b}\right)$ (in the fibre direction)

When the stiffness of the composite, matrix and filler are known, the Halpin–Tsai model can also be used to back-calculate the aspect ratio of the reinforcing particles. This will be an effective aspect ratio, because the particles can have different shapes, sizes and thicknesses, as has been pointed out in various articles [4–7]. Instead of using image analysis of TEM images to estimate the aspect ratio distribution [4,5,7], we simply use the effective aspect ratio that the model gives based on the experimental data. This effective aspect ratio is at least a reasonable estimate of the average aspect ratio [12,13] and provides a useful parameter to compare different nanocomposite compositions. The Halpin–Tsai equations predict that platelet-shaped particles are hardly effective at very low aspect ratios (<10). The maximum stiffening effect is reached only at aspect ratios above 1000 for platelets and 100 for fibres [11].

1.2. Melt rheology

In this section first the relations that are used to calculate the viscosity from the measurements will be shown. This will be followed by several equations that relate the viscosity of filled systems with the particle shape and concentration, which will be used to estimate the average particle aspect ratio.

By increasing the filler content the viscosity increases considerably in both exfoliated and intercalated nanocomposites, especially at low shear rates or low frequencies [14–18]. Unfilled polymers have usually a constant viscosity over a large frequency range with shear thinning behaviour at higher frequencies or shear rates. Nanocomposites with filler loading above a few percent show shear thinning over the entire range of frequencies [15]. The unlimited increase of the viscosity when the shear rate goes to zero is caused by the presence of a network structure in the melt that leads to a yield stress. This can be caused by the dispersed particles, which can touch or connect to each other to form a continuous structure. The formation of a network does not require a physical connection between the particles. It is sufficient that the particles feel each other's presence and are able to transfer stresses [15]. The probability that particles form a network depends on the interactions between the particles, on the shape (aspect ratio) and on the inter-particle distance. A reduction of the distance between the particles or increased aspect ratio at constant volume fraction increases the probability that the particles connect. Due to their large aspect ratio, the space the exfoliated silicate layers need to rotate freely in the melt is much larger than the volume they occupy. Therefore, the percolation threshold of exfoliated layered silicates is very low [15].

1.2.1. Flow of polymers in shear experiments

The complex shear modulus G^* is defined in oscillatory shear as:

$$\tau(t) = G^*(\omega)\gamma_0 e^{i\omega t} \tag{2}$$

$\tau(t)$, shear stress; γ_0, shear strain magnitude.

For a viscoelastic material subjected to an oscillatory strain, the oscillatory stress response will be out of phase by

an angle δ. For a perfectly elastic system $\delta = 0$, whereas for a perfectly viscous liquid, the stress is out of phase by $\delta = 90°$. For viscoelastic systems the phase angle shift is between these limiting cases.

The flow behaviour can be described by the viscosity, η. In the presence of a yield stress, τ_y, the viscosity is defined as (Bingham model):

$$\tau = \tau_{\text{yield}} + \eta\dot{\gamma} \Rightarrow \eta = \frac{\tau - \tau_{\text{yield}}}{\dot{\gamma}} \tag{3}$$

with $\dot{\gamma}$ the shear rate [s^{-1}].

The apparent yield stress (τ_{yield}) of the network can be estimated by extrapolating the stress vs. $\dot{\gamma}$ curve to zero shear rate.

A viscosity can also be determined from dynamic melt flow measurements:

$$\eta^* = \frac{G^*}{\omega} \quad \text{(complex viscosity)} \tag{4}$$

A yield stress in the melt means that flow cannot occur below a stress threshold. However, this stress is part of the measured response in the dynamic measurements and leads to an apparent increase of the measured viscosity. A corrected viscosity can subsequently be calculated by subtraction of the yield stress from the measured stress:

$$G^* = (\eta^*\omega) + \frac{\tau_{\text{yield}}}{\gamma_0} \rightarrow \eta^*_{\text{corrected}} = \frac{G^* - (\tau_{\text{yield}}/\gamma_0)}{\omega} \tag{5}$$

1.2.2. Viscosity of filled fluids

For filled systems several relations are defined between the viscosity of the unfilled fluid and the filled fluid. The relative, reduced and intrinsic viscosities are defined as:

$$\eta_{\text{relative}} = \frac{\eta}{\eta_0} \quad \text{relative viscosity} \tag{6}$$

$$\eta_{\text{reduced}} = \frac{\eta - \eta_0}{\eta_0\varphi} \quad \text{reduced viscosity} \tag{7}$$

$$[\eta] = \lim_{\varphi \to 0} \frac{\eta - \eta_0}{\eta_0\varphi} \quad \text{intrinsic viscosity} \tag{8}$$

η, viscosity of the mixture/composite (N s/m^2); η_0, viscosity of the liquid (N s/m^2); ϕ, volume fraction of particles (because in formula (7) and (8) the (dimensionless) volume fraction is used instead of the concentration, the reduced and intrinsic viscosities are also dimensionless).

1.2.3. Relations between viscosity and particle shape in filled systems

The rheology of suspensions of rigid spheres can be described by Einstein's viscosity equation (Eq. (9)). This linear equation can be used for non-settling and non-interacting spherical particles in a Newtonian liquid at low volume fractions (ϕ_{spheres}):

$$\eta = \eta_0(1 + 2.5\varphi_{\text{spheres}}) \rightarrow [\eta] \cong \eta_{\text{reduced}} = 2.5 \tag{9}$$

(at low filler fractions η_{reduced} approximates $[\eta]$).

Although polymer nanocomposites do not meet all these requirements, the filler concentrations are low and at low shear rates the melt of the polymer matrix behaves as a Newtonian fluid. Therefore, Einstein's viscosity equation (Eq. (9)) is a good basis to use with some adaptations to account for different particle shapes. The modified Einstein-type equations described hereafter can be used to describe the viscosity of nanocomposite melts. Inversely, effective aspect ratios can be estimated from melt flow measurements using these viscosity models, in a similar way as can be done using the modulus and the Halpin–Tsai equations.

Simha [19] has derived equations for small non-spherical particles, where Brownian motion has to be taken into account. The particle shape is incorporated in a factor ν, which replaces the value of 2.5 in Eq. (9). For prolate ellipsoids (~fibre shape) and oblate ellipsoids (~disk shape) different equations are derived. For these low filler concentrations a linear model is assumed, in which $\nu \cong [\eta]$.

$$\eta = \eta_0(1 + \nu\varphi_{\text{ellipsoids}}) \rightarrow \eta_{\text{reduced}} = \nu \cong [\eta] \tag{10}$$

$$[\eta] = \frac{(16/15)(a/b)}{\tan^{-1}(a/b)} \quad \text{(oblate ellipsoids—disks)}$$

$$[\eta] = \left(\frac{(a/b)^2}{15(\ln 2(a/b))} - \frac{3}{2}\right) + \left(\frac{(a/b)^2}{5(\ln 2(a/b))} - \frac{1}{2}\right) + \frac{14}{15}$$

(prolate ellipsoids—fibres)

$$[\eta] = 2.5 \quad \text{(spheres (Einstein))}$$

a, long radius in the ellipsoid; b, short radius.

The equation for $[\eta]$ for prolate ellipsoids (fibres) can be approximated by a quadratic function. For aspect ratios from 10 to 70 the best fit is:

$$[\eta] = 0.049\left(\frac{a}{b}\right)^2 + 1.12\left(\frac{a}{b}\right) - 3.74 \tag{11}$$

The equation for $[\eta]$ for oblate ellipsoids (platelets) can be approximated by a linear function for all aspect ratios:

$$[\eta] = 0.679\left(\frac{a}{b}\right) + 0.454 \tag{12}$$

Another linear equation that describes the viscosity of fluids filled with disk-shaped particles has been proposed by Luciani et al. [20]. They have studied dilute suspensions of mica flakes with various aspect ratios, and used a model proposed earlier by Kuhn [21] to describe the effect of the aspect ratio on the intrinsic viscosity of platelet filled composites. The authors simplified the model for high aspect ratios, and showed a very good fit with experimental measurements [20]:

$$[\eta] = \left(\frac{4}{9}\right) + \left(\frac{4}{3\pi}\right)\left(\frac{a}{b}\right) \quad \text{valid for : } 12 < \left(\frac{a}{b}\right) < 150 \tag{13}$$

The main difference between the results of Simha's and Kuhn's equations is the strength of the influence of the aspect

ratio. This can be seen when Eqs. (12) and (13) are compared: the factor in front of the aspect ratio is smaller in Eq. (13) than in Eq. (12). This is probably a result of the fact that the latter model (Kuhn) does not include the effect of Brownian motion. Without Brownian motion, the particles can align and the viscosity increase is less strong. Therefore, Kuhn's theory is more suitable for composites with relatively large particles, in which Brownian motion can be neglected.

A different form of a relation between the intrinsic viscosity and the particle aspect ratio of disk-shaped particles has been derived by Utracki [22]:

$$[\eta] = 2.5 + 0.025\left(1 + \left(\frac{a}{b}\right)^{1.47}\right) \tag{14}$$

Eq. (14) [22] is an exception from the linear dependence for platelets (Simha and Kuhn), as it assumes power law behaviour.

In this paper both the main advantage of the use of nanocomposites, i.e. the increased modulus, and their main disadvantage for processing, i.e. the increased viscosity, are investigated. Both are influenced by the same factors, such as particle shape and concentration. With an improved understanding of these factors, the optimum morphology can be chosen that leads to the best compromise. Nanocomposites and microcomposites with different amounts and types of fillers have been prepared, and their rheological and mechanical properties are compared. The aspect ratios of the particles were calculated from the storage modulus at room temperature using the Halpin–Tsai composite model, and from the complex viscosity in the melt using the viscosity equations proposed by Simha, Kuhn and Utracki.

2. Experimental

2.1. Materials

- Akulon® K123, injection-moulding grade PA6 from DSM, the Netherlands (M_n = 16,000, M_w = 32,000 g/mol, T_m = 220 °C) was used to produce melt-blended nano- and micro-composites.

To investigate the effect of the amount of filler and the degree of exfoliation in the nanocomposites two platelet-shaped silicates are used, both based on synthetic fluoro-mica:

- Somasif® MEE from Unicoop, Japan: synthetic mica modified with coco bis(2-hydroxyethyl) methyl ammonium surfactant.
- Somasif® ME-100 from Unicoop, Japan: unmodified water-swellable synthetic mica.

To examine the influence of the shape of the particles, the nanometer-thin platelet shaped fillers were compared to spherical and fibre-shaped fillers in the same size range:

- Snowtex® (Nissan Chemical Industries): spherical silica nanoparticles in aqueous dispersion containing 20 wt% particles with sizes between 20 and 50 nm.
- Sivomatic Sepiolite A: fibre-shaped nanoparticles. After dispersion in the polymer the particles have a length of a few hundred nm and a diameter of 10–30 nm. Sepiolite is a naturally occurring silicate mineral with a hollow channel structure, usually containing water (Fig. 1). The tubes consist of silicate layers with a similar structure as in montmorillonite or mica [23] and are connected to each other at the corners.

To study the influence of the size of the particles, the nanoparticles were compared with μm-sized glass particles of approximately the same aspect ratio.

- Sovitex Micropearls (50 20 215) spherical glass beads (average diameter 30 μm).
- Glass fibres (OCF CS 173X-10C) with an initial length of 4 mm and a diameter of 10 μm. After extrusion the length was reduced.
- Glass flakes (GF-300) with an initial diameter range of 50–1800 μm and a thickness around 2.5 μm. After extrusion the diameter was also reduced.

The silicate platelets have a modulus of 172 GPa [24]; the modulus of glass is 77 GPa [25]. The density of the silicate platelets is 2.8 g/cm^3 [26], and of glass it is 2.54 g/cm^3 [25]. The modulus and density of sepiolite are estimated from its structure. Since only approximately 50 vol% consists of the mica structure, the modulus of sepiolite is estimated to be half that of mica or montmorillonite: 86 GPa. The voids between the tubes (50 vol%) can be filled with water, and the density of non-dried sepiolite is estimated similarly to be 1.9 g/cm^3.

2.2. Specimen preparation

Mixtures of cryogenically milled polyamide-6 and filler powder were fed to a Werner and Pfleiderer ZSK 30/44 D co-rotating twin-screw extruder. The extruder was operated at 240 °C, 200 rpm, with an output rate of 10 kg/h.

To enhance the exfoliation of unmodified nano-fillers, water was injected in the extruder at 25 ml/min for the unmodified sepiolite and ME-100 [27]. The same water-assisted extrusion procedure was used for the glass microcomposites and the unfilled matrix to compare the

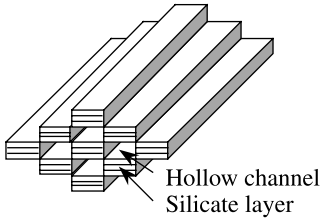

Fig. 1. The structure of sepiolite.

viscosities of the resulting composites. The dispersed silica particles (Snowtex) were injected in the extruder using a suspension in water. In this case the extruder output rate was 4 kg/h. In all these cases the water was removed using a vent at the end of the extruder. The MEE nanocomposites and the unfilled PA6 reference material were extruded without injection of water.

The samples for dynamic mechanical analysis (DMA) were 2.6 mm wide and 20 mm long. They were cut from 0.2 mm thin films, made by compression moulding of the extrudate in a Fontijne laboratory press at 240 °C. The samples were cooled in the press at an initial cooling rate of approximately 40 °C/min.

The samples for the rheological measurements were 2 mm thick and were also made by compression moulding. Al samples where dried before testing at 80 °C in vacuum for at least 2 days.

2.3. Thermo-gravimetric analysis (TGA)

A Perkin–Elmer TGA 7 thermo-gravimetric analyzer was used for the determination of the amount of surfactant on the MEE organo-silicate and the silicate content in the composites. The samples where heated in air to 800 °C, and held at that temperature for 30 min.

2.4. Optical and transmission electron microscopy

A Nikon Eclipse E600 Polarisation optical microscope was used to determine the particle size of the glass fillers. Transmission electron microscopy (TEM) was used to check the size and dispersion of the particles in the nanocomposites. Samples for TEM-analysis were prepared from extruded pellets. Films with a thickness of 70 nm were cut with a diamond knife parallel to the extrusion direction at −100 °C and observed with a Philips CM 200 TEM at an acceleration voltage of 120 kV.

2.5. Dynamic mechanical analysis (DMA)

The storage modulus in the solid state was determined with DMA using a Rheometrics Solids Analyser II at a frequency of 1 Hz (ASTM D5026). The temperature range was −130 to 200 °C, the heating rate was 5 °C/min and the length between the clamps was approximately 11 mm. The thickness of the samples was measured with an accuracy of 1 μm using a Heidenhahn MT30B thickness meter.

2.6. Rheological measurements

Dynamic rheological measurements in the melt were performed at 250 °C using a RMS 605 rheometrics mechanical spectrometer. The rheological properties of the PA6 and the nanocomposites were measured in oscillatory shear mode using 50 mm diameter parallel plates at a gap of 1.8 mm. The dynamic moduli, G' and G'', were recorded as functions of angular frequency (ω) in the range from 0.1 to 100 rad/s at a strain magnitude of 1%. PA6 can polymerize further in the melt in dry conditions [28]. All results shown are from measurements after 10 min conditioning in the melt and are corrected for the polymerisation taking place during the measurements.

3. Results and discussion

3.1. Dispersion and particle size

Optical microscopy showed that the glass fibres have an average length of approximately 200 μm after extrusion, which corresponds to aspect ratios around 20. The glass platelets have a diameter of approximately 100 μm and aspect ratios around 40 (thickness 2.5 μm).

Fig. 2 shows TEM images of PA6 nanocomposites with 5 wt% nanoparticles. ME-100 is not modified and it is not expected to exfoliate as well as silicates with an appropriate organic modification. Agglomerates varying from several to dozens of platelets are, indeed, present. For the MEE nanocomposites a much better dispersion is observed, with the majority of particles being single platelets or very small stacks. The thickness of the silicate platelets is approximate 1 nm, and the observed aspect ratio in the MEE nanocomposites is approximately 200, or less when stacks of several platelets are present. The average aspect ratio of the ME-100 nanocomposites is smaller than that of the MEE nanocomposites due to the presence of thicker stacks of platelets. The fibre shaped sepiolite shows a distribution of lengths and thicknesses of the rods with an average length of 200 nm, thickness of 10 nm, and aspect ratio around 20.

3.2. Dynamic moduli

The storage moduli of all tested micro- and nanocomposites are displayed in Figs. 3–6 as a function of temperature.

Fig. 3 shows the storage modulus for composites with 0–20 wt% of unmodified nanoplatelets (ME-100). Fig. 4 shows the same for the organically modified nanoplatelets (MEE). Higher silicate concentrations lead to a higher modulus over the entire temperature range. Note that the T_g does not change with the addition of layered silicate in these nanocomposites. The moduli of the nanocomposites with the modified MEE particles are higher than of those with the unmodified ME-100 particles, because the surface modification improves the exfoliation, leading to more individual particles with higher aspect ratios. Fig. 5 compares the moduli for various shapes of nanoparticles at 5 wt% loading. The spherical particles result in the smallest modulus enhancement. The platelet is the most effective shape because it reinforces in two directions, while the fibres just in one. Fig. 6 shows the effect of the particle shape for the micro-composites. Comparing the modulus values in Fig. 5 with those in Fig. 6, it can be seen that the

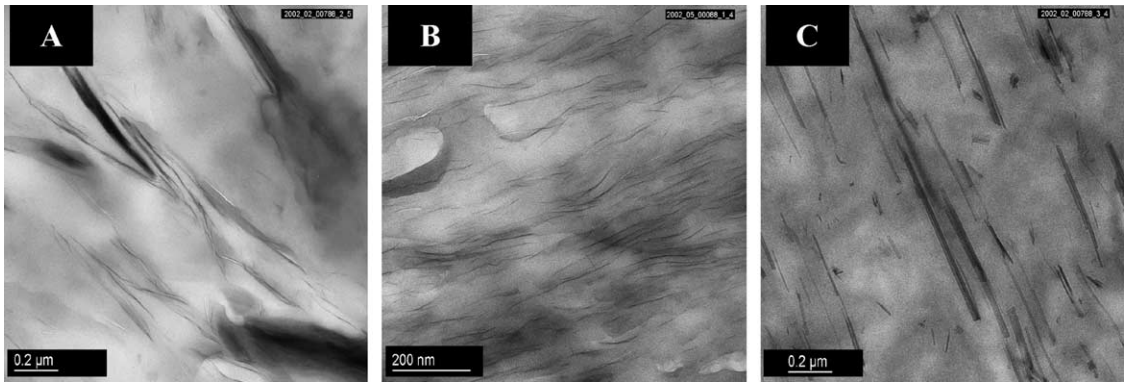

Fig. 2. TEM-images of PA6 nanocomposite with 5 wt% nanoparticles: (A) ME-100, (B) MEE, (C) sepiolite.

microparticles are less effective than the nanoparticles. Below T_g there is no significant difference in the modulus between the various shapes, probably because of the low filler content. However, above T_g the higher aspect ratio particles are more effective than the glass beads.

As already mentioned, the Halpin–Tsai equation (Eq. (1)) can be used to estimate the effective aspect ratio from composite moduli. However, there may be a small enhancement of the matrix (PA6) modulus in the nanocomposites, due to higher crystallinity induced by the large surface area of the nanoparticles. This difference will affect the estimation of the aspect ratio. To compensate for this error, the actual matrix modulus was estimated by applying the model to the 5% silica nanocomposite, of which the aspect ratio is known. The matrix modulus from this silica nanocomposite was used in the models of all other nanocomposites. For the MEE nanocomposites an additional correction was used, because a relatively large volume of surfactant was added in this case. It was assumed that the surfactant did not add stiffness to the matrix and the matrix modulus of the MEE nanocomposites could be calculated from:

$$E_{\text{matrix MEE}} = (1-\varphi_{\text{surfactant}})E_{\text{matrix nanocomposites}} \tag{15}$$

Another parameter in the composite model is the particle orientation. Because the flow during pressing of the specimen causes alignment of the particles, the platelets are assumed to be aligned in the plane of the film, while the fibres are assumed to be randomly oriented in the two major dimensions of the film. The calculated composite modulus is then [11]:

$$E_{\text{plate composite}} = E_{\text{aligned plates}} \tag{16}$$

$$E_{\text{fibre composite}} = 0.375E_{\text{aligned fibres}} + 0.625E_{\text{perpendicular}} \tag{17}$$

Despite the uncertainty in many factors such as the matrix and filler modulus, filler orientation, polydispersity and density, the effective aspect ratios could be calculated using the Halpin–Tsai composite theory and compared with calculations from rheological measurements and microscopy observations. These aspect ratios are shown in Table 1, in the column 'H–T'.

The results at very low silicate content (e.g. at 1% MEE) are very sensitive to the value of the modulus and are, therefore, not reliable. The margin of error decreases for

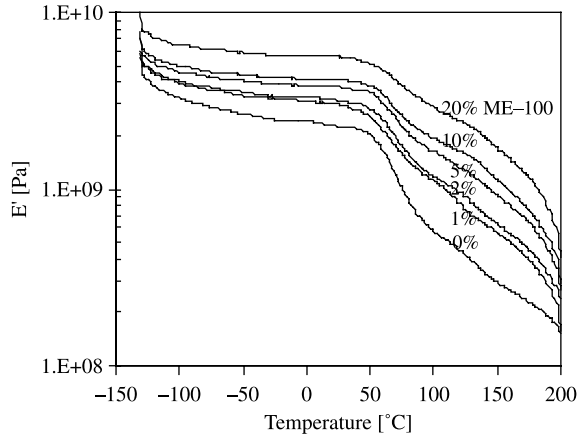

Fig. 3. The storage modulus of ME-100 nanocomposites at different volume fractions as a function of the temperature.

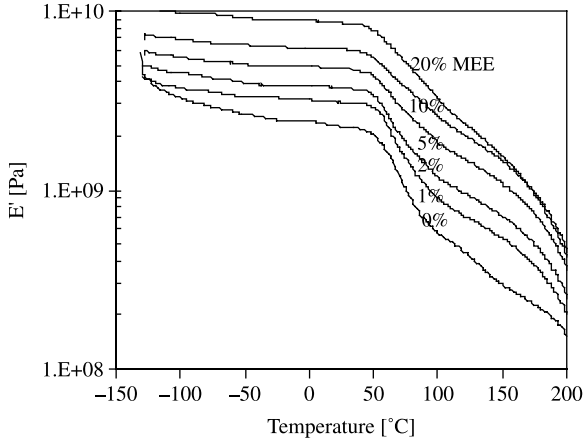

Fig. 4. The storage modulus of MEE nanocomposites at different volume fractions as a function of the temperature.

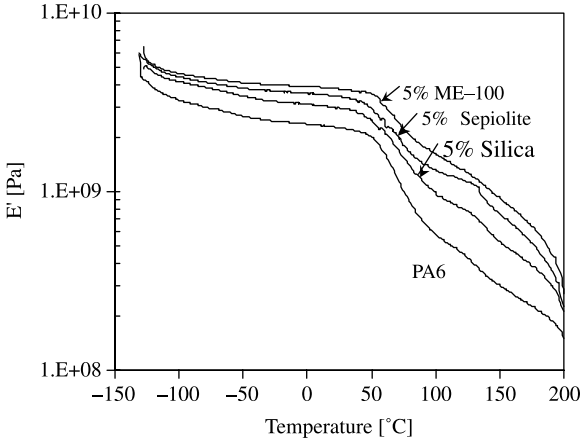

Fig. 5. The influence of the particle shape on the storage modulus of the nanocomposites.

higher filler content. The general trend from the modulus data is a decreasing aspect ratio at increasing silicate content.

3.3. Rheological tests

3.3.1. Determination of the yield stress

The complex modulus of unfilled polymers and composites without a yield stress converges to zero at zero shear frequency. However, nanocomposites with high silicate content can form a structure in the melt, which leads to a yield stress. This effect is present in the MEE nanocomposites, as can be seen in Fig. 7.

While for unfilled PA6 and low MEE volume fractions the plot in Fig. 7 shows a straight line converging to zero for $\omega \rightarrow 0$, the modulus for higher concentrations levels off to a finite value. An apparent yield stress can be determined from this value (Table 1 and Fig. 8).

A corrected viscosity, $\eta_{corrected}$, can then be calculated by subtraction of this apparent yield stress from the measured stress, using Eq. (5). The unfilled matrix and the micro-composites have zero yield stress. The nanocomposites containing unmodified particles have very low yield stresses even up to 20 wt% filler. The MEE nanocomposites show a steep increase in the yield stress above 5 wt%. At 20% MEE silicate, τ_{yield} is more than 3 decades higher than at 20 wt% ME-100. A high yield stress can be a disadvantage for applications were flows occur at low speed, such as in the impregnation of (macro-) fibre composites [29].

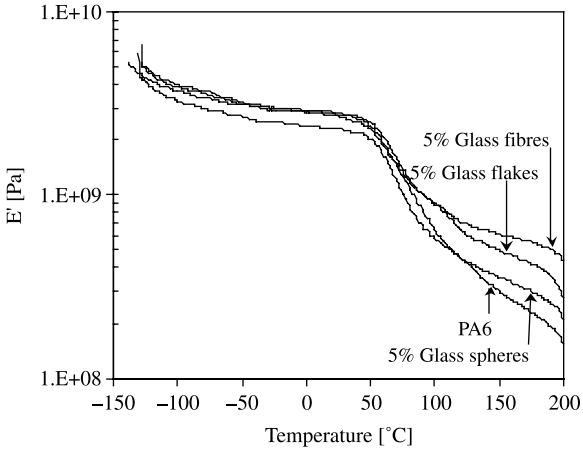

Fig. 6. The influence of the particle shape on the storage modulus of the microcomposites.

3.3.2. The influence of size and shape on the viscosity

To investigate the influence of the size and shape of the particles on the viscosity, μm-sized glass spheres, fibres and platelets with comparable aspect ratios were compared with the nm-sized unmodified particles. All data were compensated for a small viscosity increase due to some polymerisation during the measurement.

Fig. 9 shows the complex viscosity of 5 wt% composites at 250 °C. Subtraction of the apparent yield stress from the raw data results in Newtonian behaviour over a large range of frequencies. The small decrease in viscosity when glass spheres are added is probably caused by inaccuracy of the measurement. Two trends regarding the influence of the shape and the size of the particles can easily be seen in Fig. 9. The first trend is that for the same order of magnitude of the filler size (μm or nm), the fibres result in the largest increase in viscosity, closely followed by the platelets. All models described in Section 1.2 predict this effect of the aspect ratio correctly. Increasing the aspect ratio of the particles increases their effective volume fraction because high aspect ratio particles need more space to rotate and move around. The second trend is that the viscosity of the nano-composites is higher than the viscosity of the equivalent micro-composites. This is probably caused by the surface area of the nanoparticles, which is much larger than that of the microparticles, and can slow down the movement of the polymer chains due to interfacial adhesion.

3.3.3. The influence of the volume fraction

Fig. 10 shows the complex viscosity obtained from oscillatory shear measurements of ME-100 nanocomposites. The corrected viscosity shows a Newtonian plateau at low frequencies and increases linearly as a function of filler

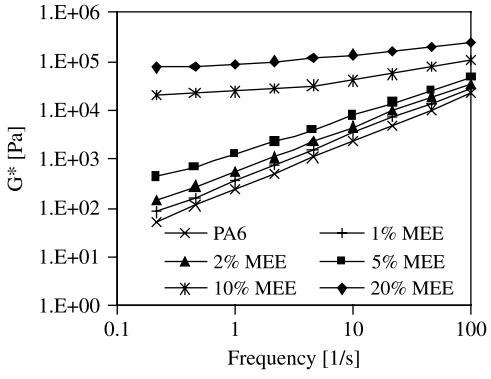

Fig. 7. Complex modulus in MEE nanocomposites.

Table 1
Apparent yield stress (τ_{yield}) and aspect ratios (*a*/*b*) calculated from the modulus (Halpin–Tsai) and the viscosity

wt%	Filler type	(*a*/*b*) H–T [9]	τ_{yield} (Pa)	(*a*/*b*) Simha oblate [19][a]	(*a*/*b*) Kuhn [21][a,b]	(*a*/*b*) Utr. [22][a,c]	(*a*/*b*) Simha prolate [19][a]
1	MEE	61[d]	0	173	277	311	
2	MEE	170	0.5				
5	MEE	111	1.5				
10	MEE	77	9.4				
20	MEE	54	99				
1	ME-100	31	0	37	59	104	
2	ME-100	28	0.2				
5	ME-100	31	0.3				
10	ME-100	17	0.2				
20	ME-100	16	0.4				
5	Glass flake	12	0	21	34	68	
5	Glass fibre	20	0				12
5	Sepiolite	20	4				20

[a] Only data at lowest filler content, because it is derived from [η].
[b] Based on linear fit (Eq. (13)) by Luciani [20].
[c] Based on power law dependence (Utracki, Eq. (14)).
[d] Large error due to low filler content, see text.

content between 0 and 20 wt% ME-100. Fig. 11 shows the same for MEE nanocomposites. The viscosity of MEE nanocomposites increases much faster with increasing silicate content compared to the ME-100 nanocomposites, with a strong acceleration above 5%. With increasing volume fraction the platelets or aggregates are more hindered in their rotation and movement, leading to a structure that can cause pseudo-solid behaviour. The high apparent yield stress at these higher concentrations (Fig. 8) is an indication of such a strong structure in the melt. When forced to flow, the nanocomposites are strongly shear thinning, because of the breaking up of the structure. After correction for the apparent yield stress, the viscosity shows a zero shear Newtonian plateau. This viscosity plateau will be used for the calculation of the aspect ratios of the particles.

3.4. Calculation of the aspect ratios from viscosity data

The aspect ratios of the particles were estimated from the complex viscosity data in the melt and were compared with those calculated from the storage modulus in the solid state and those estimated from optical microscopy or TEM. The aspect ratios (*a*/*b*) are calculated from the complex viscosities after they are corrected for the effect of the yield stress. The intrinsic viscosity is used for these calculations as a common basis for the comparison of (nano)composites with several filler types and volume fractions. For the ME-100 and MEE nanocomposites many concentrations have been tested and the intrinsic viscosity can be estimated from the intercept of the plot of $\eta_{reduced}$ vs. filler content at zero concentration (Fig. 12). A linear fit through the concentrations up to 5 wt% is used for this. The intrinsic viscosity is 25.5 for the ME-100 nanocomposites and 118 for the MEE nanocomposites, the latter is close to the value for in situ polymerized nanocomposites (105.5) found by Utracki [22]. A reasonable estimate of the intrinsic

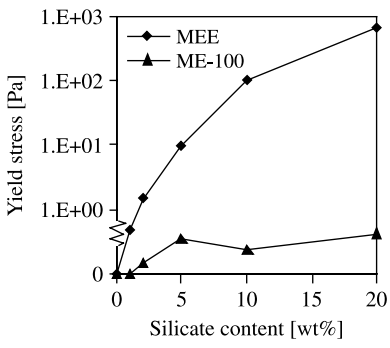

Fig. 8. The apparent melt yield stress of the MEE and ME-100 nanocomposites.

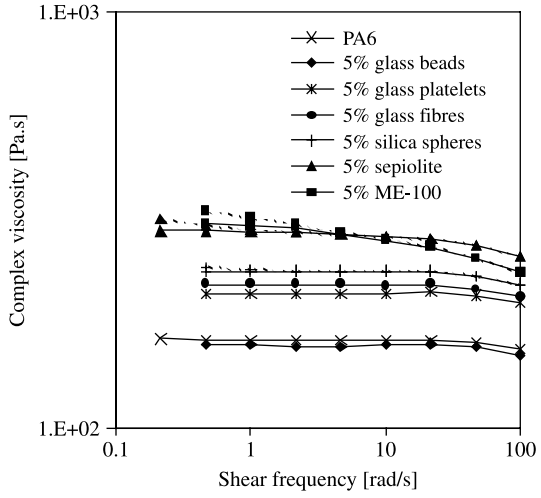

Fig. 9. Complex viscosity of 5 wt% micro- and nanocomposites at 250 °C. Dotted lines indicate as-measured viscosities (corrected for polymerisation during measurement). Solid lines indicate viscosities corrected for the yield stress.

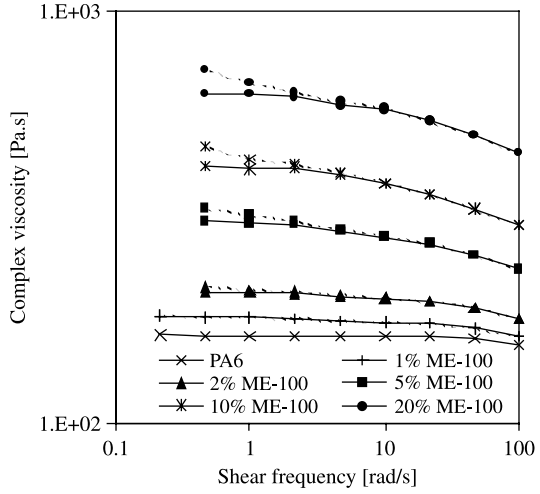

Fig. 10. Complex viscosity of PA6 ME-100 nanocomposites at 250 °C. Dotted lines indicate as-measured viscosities (corrected for polymerisation during measurement). Solid lines indicate viscosities corrected for the yield stress.

viscosity for the other composites is obtained from the reduced viscosity at 5 wt%, as it is suggested by Fig. 12.

Figure 13 shows the dependence of the intrinsic viscosity on the platelet aspect ratio described by the theory of Simha (Eq. (12)), Luciani/Kuhn (Eq. (13)) and Utracki (Eq. (14)). The two horizontal lines at 118 and 25.5 indicate the values of the intrinsic viscosity of the MEE and ME-100 nanocomposites. The intersections of these lines with the three theoretical curves determine the aspect ratios of the particles. These are shown in Table 1 together with the values estimated from the reduced viscosities for the other composites.

The viscosity model by Simha for oblate ellipsoids (platelets) predicts values of the particle aspect ratios close to the values predicted by the Halpin–Tsai composite theory for both MEE and ME-100 nanocomposites. Although it is

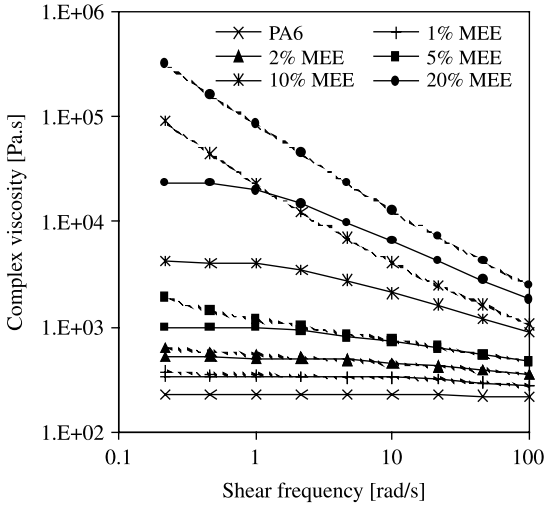

Fig. 11. Complex viscosity of PA6 MEE nanocomposites at 250 °C. Dotted lines indicate as-measured viscosities (corrected for polymerisation during measurement). Solid lines indicate viscosities corrected for the yield stress.

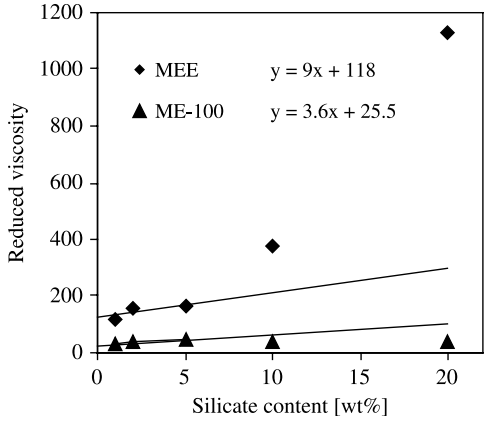

Fig. 12. Reduced viscosity MEE and ME-100 nanocomposites.

impossible to obtain accurate average particle sizes from TEM, Fig. 2 suggests that the Simha models predict reasonable aspect ratios for these nanoparticles. The viscosity theory of Kuhn/Luciani [16,17] is more suitable for relatively large particles, where Brownian motion can be ignored. It has been shown that this theory also correlates very well with experimental results from micro-scale mica composites [20]. This theory seems to overestimate the aspect ratio for nanoparticles, as well as the theory of Utracki. The increase in modulus is small for the glass filled composites, and, therefore, the error in the Halpin–Tsai results is larger in this case than in the nanocomposites. This can explain the differences between the aspect ratios calculated from the modulus and the viscosity.

The Simha viscosity model for prolate ellipsoids (Eqs. (10) and (11)) yields an aspect ratio for sepiolite close to the one of the Halpin–Tsai model and the TEM results (Fig. 2(C)). For the (micro) glass fibres the calculated aspect ratio is too low. Therefore, it appears that the Simha equation applies better for nanocomposites than for microcomposites, both for fibres and platelets.

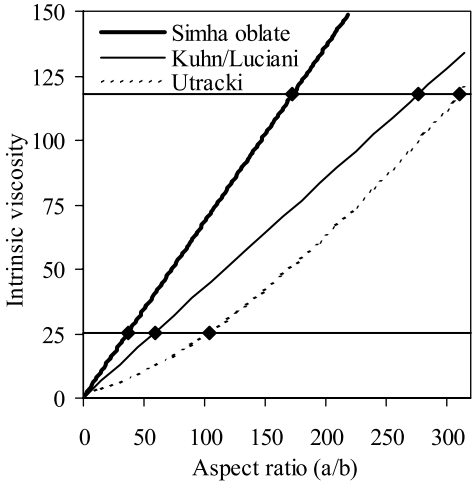

Fig. 13. Aspect ratio vs. intrinsic viscosity for platelet composites.

3.5. Comparison between the modulus increase and the viscosity increase

A comparison between the modulus increase and the viscosity increase can now be made to find the particles that provide the best compromise for specific applications. Instead of only focussing on the reinforcing efficiency of the particles, as discussed previously (Figs. 3 and 4), here we will consider the modulus increase in relation to the viscosity of the melt. This is obviously important for the processability of the material. The modulus increase compared to the viscosity increase is shown by plotting the relative modulus ($E_{composite}/E_{matrix}$) at room temperature vs. the relative viscosity in the melt, shown in Fig. 14 for two shear frequencies: 'low' (0.46 rad/s, Fig. 14(A)) and 'high' (100 rad/s, Fig. 14(B)).

All relative viscosities are based on the complex viscosities calculated without subtraction of the yield stress, because this is more representative for the forces in processing equipment. Fig. 14(A) shows that the curve for unmodified silicate (ME-100) has a slightly higher slope than the one of the modified silicate (MEE). This indicates a tendency of the unmodified silicate to result in a lower viscosity increase at low shear rates for the same modulus increase, especially at higher volume fractions, although larger amounts of silicate are needed. The advantage becomes even clearer when also the yield stress is considered (Fig. 8); this is up to two decades lower for a similar modulus increase. On the other hand, there is no such tendency at high shear rates (Fig. 14(B)): the slope is the same here for both types of reinforcement. When high shear rate processes are applied, e.g. injection moulding, the penalty in the viscosity for better exfoliation is reduced, probably because the platelets become aligned.

The fibre shaped sepiolite nanofiller causes a larger increase of the viscosity than the platelet filler at a similar modulus increase at high shear rates. This is supported by the theories, which predict a quadratic dependence of the viscosity on the aspect ratio for fibres influenced by Brownian motion, and a linear dependence for platelets. The solid-state modulus predicted by the Halpin–Tsai model shows a linear dependence for all shapes.

A remark is due here on the effect of the particle size on the viscosity, which can be seen in Fig. 9. When nanofillers are used, there is a much larger surface area available for interactions between the particles and the polymer melt. It can be expected that these interactions add a contribution to the friction between the particles and the matrix and, thus, increase the viscosity. In addition, a thin layer of adsorbed polymer chains on the surface can also lead to an effective increase of the volume fraction of particles, which would only be significant when the filler particles are in the nanometer range. The simple hydrodynamics-based Einstein-type viscosity models do not take these effects into account. For the same volume fraction of particles, the interfacial surface depends on the size of the particles. This additional term to the viscosity becomes important when the size of the particles is very small and it may explain some of the differences in the viscosity in Fig. 9 between the nanocomposites and the microcomposites at the same volume fractions and particle shapes.

4. Conclusions

Nanocomposites show higher moduli in the solid state at low filler content than traditional glass micro-composites. This increased modulus is accompanied by a strong increase in melt viscosity. The particle shape and aspect ratio have a strong influence on both the modulus in the solid state and the melt viscosity. The modulus increase is higher for platelets than for fibres for the same volume fraction, because the platelets reinforce in two directions instead of one. The viscosity increases less for platelets than for fibres. This is accounted for by the viscosity theories, which predict a linear dependence on the aspect ratio for platelets and a quadratic one for fibres. The nanocomposites produced with unmodified nano-platelets have a lower modulus and a lower viscosity than those based on organically modified platelets when the same fraction of silicate is considered. The experimental data in combination with the models based on the room

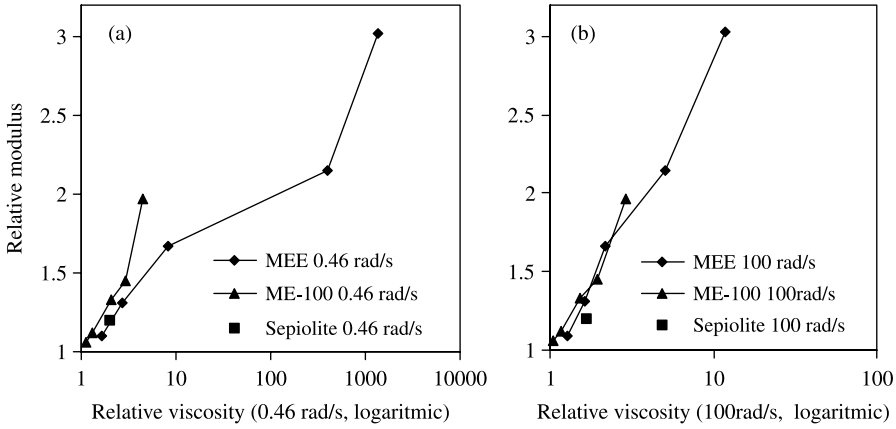

Fig. 14. Relative modulus compared with relative viscosity (uncorrected for yield stress): (a) 0.46 rad/s, (b) 100 rad/s.

temperature modulus or on the melt viscosity result in an effective aspect ratio for the unmodified silicate of approximately 1/4 of the modified silicate. This is due to the larger amount of multi-platelet stacks in the unmodified silicate nanocomposite, which were also observed in TEM images. In modified silicate nanocomposites the melt yield stress increases rapidly above 5 wt% silicate, suggesting a strong structure of interacting particles. In contrast, the unmodified particles do not lead to a large yield stress, even up to 20 wt% filler.

The Simha theory for oblate and prolate spheroids predicts platelet aspect ratios from melt viscosity data that are close to the results from the Halpin–Tsai model for nanocomposites. For the glass microcomposites the theory of Kuhn [21], which does not include the effect of Brownian motion, is more accurate.

When the advantage in mechanical properties (the increased modulus) is compared with the disadvantage of the increased viscosity and yield stress in the melt, it is clear that the choice for the best filler type depends on the type of process that is used to make the composite. For low shear rate processes, such as fibre impregnation and wetting, the nanocomposites based on partially exfoliated unmodified silicate have the advantage of a lower viscosity and a much lower yield stress (or no yield stress at all at low filler content) compared to those based on modified silicate when the same modulus enhancement is considered. However, for high shear rate processes, such as injection moulding, both types of nanocomposite show a similar increase in viscosity, probably because the platelets can align in fast flow fields. In this case the higher efficiency of modulus enhancement of the modified platelets could be the determining criterion. For film blowing this high viscosity can be an advantage, similar to high MW polymers. When comparing unmodified silicate (processed in this specific way to enhance the exfoliation [27]) with modified silicate, it is clear that the modified silicate is more efficient: approximately twice as much unmodified silicate than modified silicate has to be added to reach the same modulus. However, while twice the amount of silicate is needed, it has to be pointed out that all the filler that is added is effective as reinforcement. In the case of modified silicate up to 40 wt% of the added filler material (known as organoclay) consists of the organic modification, which does not increase the modulus, and could even have a negative influence. In other words, on the basis of the weight of added filler there is not so much difference. In addition, the price of unmodified filler might be lower because the modification is not applied, and the thermal stability of the nanofiller will be much better because it does not contain a temperature sensitive surfactant.

Acknowledgements

The work of D.P.N. Vlasveld, A.D Gotsis and S.J. Picken forms part of the research program of the Dutch Polymer Institute (DPI), project number 279. The authors would like to thank DSM Research for the help with the extrusion of the composites and especially H. Geesink for his help in this research.

References

[1] Kojima Y, Usuki A, Kawasumi M, Okada A, Fukushima Y, Kurauchi T, et al. J Mater Res 1993;8(5):1185–9.
[2] Usuki A, Kawasumi M, Kojima Y, Okada A, Kurauchi T, Kamigaito O. J Mater Res 1993;8(5):1174–8.
[3] Usuki A, Kojima Y, Kawasumi M, Okada A, Fukushima Y, Kurauchi T, et al. J Mater Res 1993;8(5):1179–84.
[4] Fornes TD, Paul DR. Polymer 2003;44(17):4993–5013.
[5] Kuelpmann A, Osman MA, Kocher L, Suter UW. Polymer 2005; 46(2):523–30.
[6] Wu YP, Jia QX, Yu DS, Zhang LQ. Polym Test 2004;23(8):903–9.
[7] Sheng N, Boyce MC, Parks DM, Rutledge GC, Abes JI, Cohen RE. Polymer 2004;45(2):487–506.
[8] van Es M, Xiqiao F, van Turnhout J, van der Giessen E. Comparing polymer-clay nanocomposites with conventional composites using composite modeling. Specialty polymer additives. Oxford: Blackwell Science; 2001.
[9] Halpin JC, Kardos JL. Polym Eng Sci 1976;16(5):344–52.
[10] Halpin JC. J Compos Mater 1969;3:732–4.
[11] van Es M. Polymer clay nanocomposites. The importance of particle dimensions. Thesis, Delft University of Technology; 2001.
[12] Vlasveld DPN, Groenewold J, Bersee HEN, Mendes E, Picken SJ. Polymer 2005;46(16):6102–13.
[13] Vlasveld DPN, Bersee HEN, Picken SJ. Moisture absorbtion in polyamide-6 silicate nanocomposites and its influence on the mechanical properties. Polymer, Submitted for publication.
[14] Hoffmann B, Kressler J, Stoppelmann G, Friedrich C, Kim GM. Colloid Polym Sci 2000;278(7):629–36.
[15] Krishnamoorti R, Yurekli K. Curr Opin Colloid Interface Sci 2001; 6(5–6):464–70.
[16] Krishnamoorti R, Giannelis EP. Macromolecules 1997;30(14): 4097–102.
[17] Giannelis EP, Krishnamoorti R, Manias E. Adv Polym Sci 1999;138: 107–47.
[18] Solomon MJ. Macromolecules 2001;34:1864–72.
[19] Simha R. J Phys Chem 1940;44:25–34.
[20] Luciani A, Leterrier Y, Manson JAE. Rheol Acta 1999;38(5): 437–42.
[21] Kuhn W, Kuhn H. Helvetica Chimica Acta 1945;28(1):97–127.
[22] Utracki LA, Lyngaae-Jorgensen J. Rheol Acta 2002;41(5): 394–407.
[23] Ruiz-Hitzky E. J Mater Chem 2001;11(1):86–91.
[24] Shell HR, Ivey KH. Fluorine micas: Bureau of mines. Washington DC: US Department of the Interior; 1969.
[25] Hull D, Clyne TW. An introduction to composite materials 1996. Cambridge: Cambridge University Press.
[26] Rothon R. Particulate-filled polymer composites. London: Longman; 1995.
[27] Korbee R. Process for the preparation of polyamide nanocomposite composition. NL Patent WO 99/29767 DSM; 1999.
[28] Kohan MI. Nylon plastics handbook. Munich: Carl Hanser Verlag; 1995.
[29] Vlasveld DPN, Parlevliet PP, Bersee HEN, Picken SJ. Compos Part A: Appl Sci Manufact 2005;36(1):1–11.